Experimental verification of shock sterilization for marine Vibrio sp using microbubbles interacting with underwater shock waves

Wang, Jingzhu

Abe, Akihisa

(Citation)
Journal of Marine Science and Technology,21(4):679-688

(Issue Date)
2016-12

(Resource Type)
journal article

(Version)
Accepted Manuscript

Experimental Verification of Shock Sterilization for Marine *Vibrio* sp. using Microbubbles Interacting with Underwater Shock Waves

Jingzhu Wang and Akihisa Abe*

Graduate School of Maritime Sciences, Kobe University, 5-1-1 Fukaeminami-machi,

Higashinada-ku, Kobe 658-0022, Hyogo, Japan

*Tel. & fax number: 078-431-6277. E-mail: a-abe@maritime.kobe-u.ac.jp

Abstract

In this paper, shock sterilization using the motion of microbubbles induced by underwater shock waves is verified experimentally. A bio-experiment is carried out using marine *Vibrio* sp.. Underwater shock waves are produced by electric discharge in a semi-ellipsoidal discharge reflector. The shock waves are focused to increase the pressure the generated microbubbles are exposed to. The microbubbles are generated independently. The microbubble generator can produce microbubbles of around 50 μm diameter by means of Kelvin-Helmholz instability and Venturi effect. Propagation behavior of shock waves and the generation process of microbubbles are captured by high speed camera. The experimental results show that the supply of microbubbles increases the potential of shock sterilization. In addition, it is found that shock waves without microbubbles also have the capacity of sterilization, and this means that cavitation bubbles generated behind converging shock waves contribute to inactivating marine bacteria.

Key words: Experimental verification, Underwater shock wave, Microbubble, Sterilization effect

1 Introduction

The problem of ships ballast water has become a serious issue of sea traffic in recent years. International Maritime Organization (IMO) reported that 30-50 hundred million tons of ships ballast water is in use all over the world every year. A ship carries ballast water containing marine bacteria from one port to another, and the released species from a ship may damage local marine ecology systems. Accordingly, IMO in 2004, adopted the international convention for the control and management of ships' ballast water and sediments, to minimize and ultimately eliminate the risks to the environment, human health, property and resources arising out of the transfer of adventive aquatic organisms and pathogens [1]. To satisfy the stringent regulations for the discharge of ships ballast water, treatment systems, installed in vessels, have been developing worldwide. These technologies can be categorized as mechanical, physical and chemical methods [2]. However, when we consider only the treatment of marine bacteria, there is still room for improvement in the sterilizing treatment in terms of ease of operation, cost, efficiency, and safety. Abe et al. in 2010 [3] proposed environment-friendly shock sterilization of marine bacteria using the collapsing motion of microbubbles induced by underwater shock waves without any chemicals. They investigated the tolerance of marine *Vibrio* sp. exposed to shock pressures using a gas gun, and found that marine *Vibrio* sp. was sterilized at 200 MPa, the pressure behind a reflected shock wave. Furthermore, they observed the interaction of the microbubbles with the underwater shock waves generated by explosions of 10 mg of AgN_3, and pointed out the maintenance of a strong pressure vibration with a magnitude of 200 MPa for about 20 μs at a distance of 20 mm from the explosion center [4]. These results suggested that rebound shock waves generated by the microbubble motion have sufficient potential to sterilize marine bacteria.

The microbubble is defined as a bubble with a diameter less than 50 μm in the present paper. Microbubbles have recently been applied to new technologies due to such unique properties as having a larger surface area to volume ratio, slower rising velocity in liquid phase, and production of free radicals by self-contraction [5]. Takahashi et al. [6] detected the generation of free radicals caused by ionic accumulation on the surface of contracting microbubbles without any external pressure. Recently, microbubbles have also been applied in the fields of molecular imaging and waste water treatment. Kaufmann [7] and Morawski [8] have investigated a molecular imaging technique, using site-targeted microbubble contrast agents, to develop a sensitive and specific diagnostic approach for the early detection of disease and analysis of disease progression. Chu et al. [9] performed experiments using micro and macro bubbles in an

ozonation system of water purification and sewage treatment, respectively. They found that microbubbles could increase the mass transfer rate of ozone and enhance total organic carbon removal efficiency.

The present study aims to develop a shock sterilization method for marine bacteria using interaction of microbubbles with underwater shock waves [3]. The concept of the sterilization method is as follows: at the first stage, floating microbubbles in water containing marine bacteria start to contract just after they are exposed to an external underwater shock wave. At the second stage, free radicals, that can strongly oxidize marine bacteria, are produced due to the condensation of the surface ionic charge from the contraction of the microbubbles. At the final stage, microbubbles expand and generate rebound shock waves. The marine bacteria near a microbubble are killed by free radicals and the strong pressure of rebound shock waves. This method can probably make marine bacteria inactivate physically and biochemically, so that the shock sterilization method would be an extremely safe and better technique for marine ecosystems.

The present paper reports on experimental verification of a shock sterilization method using microbubble-shock wave interaction. In order to investigate the sterilization effect, marine *Vibrio* sp. was used. Underwater shock waves were produced by an electric power supply, and pressure increase was managed using a semi-ellipsoidal reflector. Microbubbles were supplied using the original microbubble generator. Propagation behavior of underwater shock waves and the generation process of microbubbles were investigated by optical observation. Furthermore, in consideration of cavitation bubbles behind the converging underwater shock waves, the sterilizing potential of the present experimental device was investigated and the effects of the shock sterilization method were examined to obtain higher performance.

2 Bio-experiment

Figure 1 shows the experimental setup for the bio-experiment. The experimental device consists of a test chamber including a two-dimensional semi-ellipsoidal discharge section and targeted section, a water tank with a microbubble generator, a pump (MD-6ZK-N, Iwaki Inc., 6 l/min) providing a circular flow and supplying water to the microbubble generator, and an electric power supply (HPS 18K-A, Tamaoki Electronics Co-Ltd). The inside dimensions of the test chamber were 500 mm long by 30 mm wide by 10 mm depth, and those of the water tank were 200 mm diam. by 250 mm height. As shown in this figure, the semi-ellipsoidal discharge chamber can effectively focus shock wave exposure to the flow in the targeted section [10]. The output power of the electric discharge is about 28.7 kV at the 1st focal point. The frequency of the electric discharge was 1 Hz, and the total volume of artificial seawater with cell suspension circulated in the device was 4 l.

2.1 Two-dimensional Semi-Ellipsoidal Electric Discharge Chamber

Shock focusing using a semi-ellipsoidal reflector was introduced to enhance the shock pressures in the flow channel, as shown in Fig. 2. The shape of the reflector is half of an ellipse, the major axis and the minor axis are 70 mm and 50 mm, respectively. The distance between two focal points is 50 mm. The dimensions of the reflector are 50 mm in height by 35 mm in width by 10 mm depth. A silicone film was used to prevent marine bacteria getting into the electric discharge section. There are two slots in the upper side of the electric discharge section to exhaust air produced by electric discharge.

2.2 Original Microbubble Generator

In general, microbubbles are fundamentally produced by decompression of air-saturated solution and electrolysis of water. Hasegawa et al. [11] used a pipe with slits causing local shear stress to the flow and produced 40-50 μm diameter microbubbles. Based on the study by Hasegawa, we devised a new style of microbubble generator designed and produced using a pipe with bores. Figure 4 shows a schematic diagram of the microbubble generator. Two types of acrylic pipes were prepared. Type-A pipe, for observation of microbubble formation, has a thickness of 1 mm and an inner diameter of 6 mm with 44 bores 1 mm in diameter, while the type-B pipe used for bio-experiment has a thickness of 0.5 mm and an inner diameter of 6 mm with 288 bores 0.5 mm in diameter. The pipes were connected to a three-way pipe that has air and water conduits. The air supply tube was rubber with an inner diameter of 2 mm and a thickness of 1 mm. Water is supplied by a pump, and air is drawn into the acrylic pipe due to the pressure decrease generated by water flow, as shown in Fig. 3. Bubbles are generated by instability of the water–air interface, and torn into tiny bubbles when they pass through the bores. Thus, microbubbles are produced by shear flow and pressure change in the bores. The supplied water volume of the pump was 6 l/min, and the air intake volume was about 33 ml/min. The diameters of the microbubbles generated by two generators were measured from the observation images taken by a single-lens reflex digital camera (D2X, Nikon Co. Ltd.).

2.3 Cell Experiment

A solution of marine *Vibrio* sp., isolated from seawater, was used as the bio-experiment specimen. Marine *Vibrio* sp. belongs to the same genus as *cholera* but has no virulence. In the cell experiment, about 10^9 cfu/ml marine *Vibrio* sp. was first put into artificial seawater and diluted to about 10^6 cfu/ml. Samples were extracted from the solution in the test chamber every 30 minutes to check the cell viability ratio during the application of the incident shock pressure to the microbubbles. Next, the cell suspension was diluted serially and then spread on agar plates. The plates were incubated for 24 hours and colonies grown on the agar plate as shown in Fig. 4 were counted. The total number of colony-forming cells in 1 ml was evaluated on the basis of the dilution ratio of the cell suspension and the number of colonies on the plate.

3 Results and Discussion

3.1 Propagation Behaviors of Shock Wave

Figure 5 shows sequential images of the propagation and focus process of an underwater shock wave in the discharge chamber using schlieren method. The resolution is 320 × 232 pixels, the framing speed is 500 kfps, and the exposure time is 200 ns. In order to fasten the electrodes, two square acrylic plates shown in Fig. 5 (1) were used to hold the electrodes. The bow shadow of the 1st shock wave (1st SW) was observed in the electric discharge chamber in Fig. 5 (2). In addition, the reflected shock wave (RSW) from the semi-ellipsoidal wall was also observed. In Fig. 5 (3) and (4), the 1st SW propagates into the flow channel passing though the silicone film. RSW is converging at the 2nd focal point in Fig. 5 (5). In Fig. 5 (3)-(5), it was found that the shape of RSW deteriorated because of the slots of the electric discharge chamber and silicone film. After RSW converged, it impinged against the reflected 1st shock (RSW1) wave from the right end wall of the test chamber in Fig. 5 (6). RSW also reflected on the right end wall, and propagated to the left as RSW2.

3.2 Microbubble Formation from Original Bubble Generator

The process of microbubble generation by the type-A generator was observed by a high-speed camera, the conditions of which were 3000 fps and 100 μs exposure time. Figure 6 shows sequential images of the microbubbles produced. Figure 6 (2) is an image just after the pump starts, where air sucked into the generator is observed at the end of air supply tube. In Fig. 6 (3), disruption of the sucked air is observed, and bubbles generated by the instability of air-water interface are moving left with the water flow. Figure 6 (4)-(6) show how bubbles go outside from the bores and are diffused in the water tank. In Fig. 6 (6), we can clearly see that the air-water interface develops to be about 4 mm long from the end of the air supply tube.

In order to observe the change of air-water interface near the exit of the air supply tube, a magnified observation was carried out under the same conditions as in Fig. 6. The magnified area is shown in the boxed area in Fig. 7 (a). The interface between water and the mass of sucked air from the air supply tube is vibrated by Kelvin-Helmholtz instability [12], and various sizes of bubbles are produced as shown in Figs. 7 (b) and (c). The bubble diameters were about 300 μm to 500 μm.

The behaviors of bubbles that pass through the bores of the generator vary due to their initial sizes. Figure 8 shows the breakup of a bubble passing through a 1 mm diameter bore. The large bubble shown in Fig. 8 (1) was torn into two bubbles as it passed through a 1 mm bore, as shown in Fig. 8 (2) and (3). In Fig. 8 (3)-(6), we see how a bubble passing through the pipe wall extended into a cylindrical shape and then some smaller bubbles about 100 μm were torn from it.

Figure 9 shows the breakup of smaller bubbles passing through a 1 mm bore. The bubbles were not torn as they entered the bore. In Fig. 9 (a), a bubble with a diameter just less than 1 mm expanded into a cylindrical shape and was then torn into some smaller bubbles after it passed through the bore. On the other hand, in Fig. 9 (b) a bubble passes through the bore without breakup. However, in this case, the diameter of bubble was quite equal to the bore diameter.

In the process of microbubble generation of the present device, bore diameter is considered to be the important parameter affecting the size of microbubbles. Therefore, diameter distributions of microbubbles generated by 0.5 mm diam. bore (type-B) were investigated. Figure 10 shows the relationship between production rate and microbubble

diameter of type-A and B bubble generators. The bubbles were observed using a single-lens reflex digital camera in the targeted section shown in Fig. 1. The mean diameter of the bubbles from type-A and type-B generators was about 90 μm and 50 μm, respectively. Abe et al. have analyzed the rebound pressures of the collapsing microbubbles by solving Herring bubble motion equations with the experimental pressure profile of the incident shock wave [13]. It is apparent that the rebound shock pressure of a 50 μm diam. bubble will be higher than that of a 90 μm diam. bubble. Consequently, the bio-experiments were carried out using the type-B microbubble generator.

3.3 Potential of the Sterilization using Microbubble-Shock Wave Interaction

Figure 11 shows magnified images of the interaction between microbubbles and underwater shock waves in the targeted section shown in Fig.1. The underwater shock wave produced by electric discharge propagated from the left to the right in the image. The shadows of microbubbles could not be observed clearly because of their small size in Fig. 11 (a). However, Fig.11 (b) shows a lot of microbubble shadows due to expansion of the microbubbles as they interacted with the shock wave.

Figure 12 shows the estimations of the number of viable cells from the bio-experiments. Solid squares, open diamonds, solid triangles, and open circles represent experimental results under the condition of only circulation (condition 1), the condition of circulation with microbubbles (condition 2), the condition of circulation with shock waves (condition 3), and the condition of circulation with microbubbles and shock waves (condition 4), respectively. It was found that marine bacteria were hardly affected under conditions 1 and 2. On the other hand, sterilization effects were clearly obtained under conditions 3 and 4. These results show that the reduction rates of viable cells are about 46% and 69% per hour, respectively. If the trend of this experimental data is maintained, it is estimated that condition 4 will see a 99.99% reduction of the viability ratio in 8 hours. The differences in the results between the conditions of 3 and 4 are the sterilization effects induced only by the motions of microbubbles. It is hard to believe that the sterilization effect obtained under condition 3 was possible because microbubbles are not introduced and the peak pressure of the incident shock wave was only around 10 MPa. Contributions of bubbles are considered to be necessary for killing bacteria.

It is well known that cavitation bubbles are produced behind converging underwater shock waves. In addition, it has also been reported that cavitation bubbles are generated by expansion waves resulting from the stress waves that propagate from wall material in a narrow chamber [14]. Observation of cavitation bubbles was carried out using high speed camera in schlieren method. Figure 13 shows sequential images of generation and collapse of cavitation bubbles in the test chamber. The resolution is 512 × 384 pixels, the framing speed is 500 kfps, and the exposure time is 200 ns. The 1st SW was propagating and RSW were converging at 2nd focal point in Fig. 13 (1)-(3). Shadows of expanding cavitation bubbles were clearly observed in the semi-ellipsoidal reflector due to the interaction with RSW in Fig. 13 (5)-(9). Although cavitation bubbles are not directly found behind RSW in the flow channel, existence of bubbles is confirmed by their expansion shown in Fig. 13 (9)-(12).

Figure 14 shows magnified observation on collapse of cavitation bubbles produced by converging underwater shock waves. The resolution is 320 × 98 pixels, the framing speed is 500 kfps, and the exposure time is 200 ns. The rebound shock wave generated by collapse of cavitation bubble was observed in Fig. 14 (3) and (4).

Diameter distributions of cavitation bubbles generated by underwater shock waves in the flow channel are shown in Fig. 15. These results were measured using an optical image taken 30 minutes after the start of electric discharges. Bubble diameters are broadly scattered from 10 μm to 200 μm. From the results, the sterilization effect under condition 3 was considered to be caused by the collapse of cavitation bubbles produced by converging underwater shock waves. However, this suggests that cavitation bubbles of various sizes cause weak sterilization effects on marine bacteria.

4 Conclusions

The study aims to develop an environment-friendly sterilizing treatment technique for marine bacteria using microbubbles interacting with underwater shock waves. In the present paper, bio-experiments were carried out using marine *Vibrio* sp. to investigate the potential of shock sterilization. Original bubble generators were developed to provide microbubbles. The pressure increase of the incident shock wave was achieved by focusing the shock waves produced by underwater electric discharge in the semi-ellipsoidal reflector. The propagation behaviors of shock waves and generation process of microbubbles were observed by high speed camera. In the original microbubble generator, bubbles were generated by instability of the water–air interface, and torn into smaller bubbles when they passed through the small bores. Using the present bubble generator, mean bubble diameters of 50 μm were produced. On the other hand, the underwater shock wave generated at the 1st focal point of the semi-ellipsoidal reflector reflected on the inner wall of

the reflector and converged at the 2nd focal point. From the bio-experimental results, 46% and 69% of the marine bacteria were killed in an hour under the conditions of circulation with shock waves and circulation with microbubbles and shock waves, respectively. It was confirmed that cavitation bubbles were generated behind the converging shock waves by observing optically the propagation of shock waves. The collapse of cavitation bubbles was proven to be capable of inactivating marine bacteria. However, because of the various sizes of cavitation bubbles, strong sterilization effects were not obtained using only shock waves.

Acknowledgements

This work was supported by JSPS KAKENHI Grant Number 25630405.

References

[1] International Maritime Organization, "Adoption of International Convention for the Control and Management of Ships' Ballast Water and Sediments," International Conference on Ballast Water Management for Ships, Agenda Item 8, 16 February 2004.

[2] Tsolaki E, Aiamadopoulos E (2010) Technologies for ballast water treatment: A review. Journal of Chemical Technology and Biotechnology 85:19–32

[3] Abe A, Mimura H, Ishida H, Yoshida K (2007) The effect of shock pressures on the inactivation of a marine *Vibrio* sp.. Shock Waves 17:143–151

[4] Abe A (2010) Pressure generation from micro-bubble collapse at shock wave loading. Journal of Fluid Science and Technology 6: 235–246

[5] Xu Q, Nakajima M, Liu Z, Shiina T (2011) Biosurfactants for microbubble preparation and application. International Journal of Molecular Sciences 12:462-475

[6] Takahashi M, Chiba K, Li P (2006) Free-Radical generation from collapsing microbubbles in the absence of a dynamic stimulus. Journal of Physical Chemistry B 111:1343-1347

[7] Beat A Kaufmann, Jonathan R Lindner (2007) Molecular imaging with targeted contrast ultrasound. Current Option in Biotechnology 18:11-16.

[8] Anne M Morawski, Gregory A Lanza, Samuel A Wickline (2005) Targeted contrast agents for magnetic tesonance imaging and ultrasound. Current Option in Biotechnology 16:89-92.

[9] Libing Chu, Xinhui Xing, Anfeng Yu, Yunan Zhou, Xulin Sun, Benjamin Jurcik (2005) Enhanced ozonation of simulated dyestuff wastewater by microbubbles. Current Option in Biotechnology 16:89-92.

[10] Nobuhito Tsujii, Biyu Wan, Haruo Mimara, Akihisa Abe (2012) Experimental study on inactivation of marine bacteria using electrodischarge shock wave. *28th International Symposium on Shock Waves* 2:915-921.

[11] Hiroaki Hasegawa, Yasuhiro Masaki, Kazuo Matsuuchi, Yusuke Yoshida (2006) Microbubble generation by using pipe with slits. The Japan Society of Mechanical Engineers 72:160-166.

[12] John W. Miles (1959) On the Generation of surface waves by shear flows part 3. kelvin-helmhotz instability. Journal of Fluid Mechanics 6:pp583-598.

[13] Abe A, Wang J, Shioda M, Maeno A (2014) Observation and analysis of interactive phenomena between microbubble and underwater shock wave. Journal of Visualization, DOI 10.1007/s12650-014-0257-7.

[14] Koita Taketashi, Sun Mingyu (2014) Visualization of underwater shock wave and bubble phenomena induced by electric discharge in a narrow water tank. Proceedings of Shock Waves Symposium pp134-135.

Fig. 1 Schematic diagram of experimental setup for bio-experiment

Fig. 2 Schematic diagram and photo of the two-dimensional ellipsoidal electric discharge chamber with flow channel

Fig. 3 Schematic diagram of a microbubble generator

Fig. 4 Colonies of marine *Vibrio* sp. on an agar plate

Fig. 5 Sequential images of generation and propagation process of underwater shock wave in the discharge chamber and the test chamber using schlieren method

Fig. 6 Sequential images of microbubbles produced by the type-A original bubble generator

Fig. 7 Magnified observation of motion of the air-water interface

Fig. 8 Breakup of a large bubble passing through a 1 mm bore

Fig. 9 Behavior of bubbles passing through a bore:

(a) Breakup of bubbles (b) A bubble passing through a bore

Fig. 10 Diameter distributions of bubbles generated by the original devices

Fig. 11 Interaction between microbubbles and underwater shock waves:

before introduction of an underwater shock wave (a), and after introduction of shock wave (b)

Fig. 12 Estimation of the number of the viable cells:

circulation only■, circulation with microbubbles ◇, circulation with shock waves ▲, and circulation with microbubbles and shock waves ○

Fig. 13 Sequential images of observation of cavitation bubbles behind converging underwater shock waves

Fig. 14 Observation on collapsing motion of cavitation bubble in the test chamber

Fig. 15 Diameter distributions of cavitation bubbles generated by underwater shock waves in the flow channel

Figure

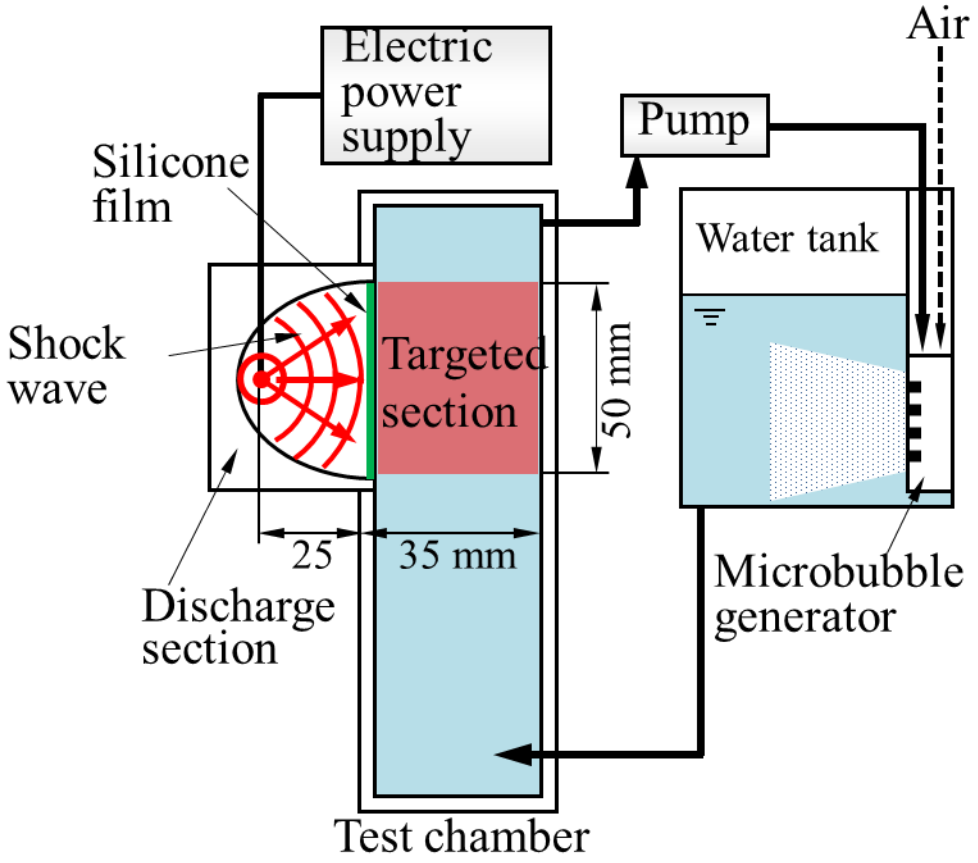
Air
Electric power supply
Pump
Silicone film
Water tank
Shock wave
Targeted section
50 mm
25
35 mm
Discharge section
Microbubble generator
Test chamber

Fig. 1

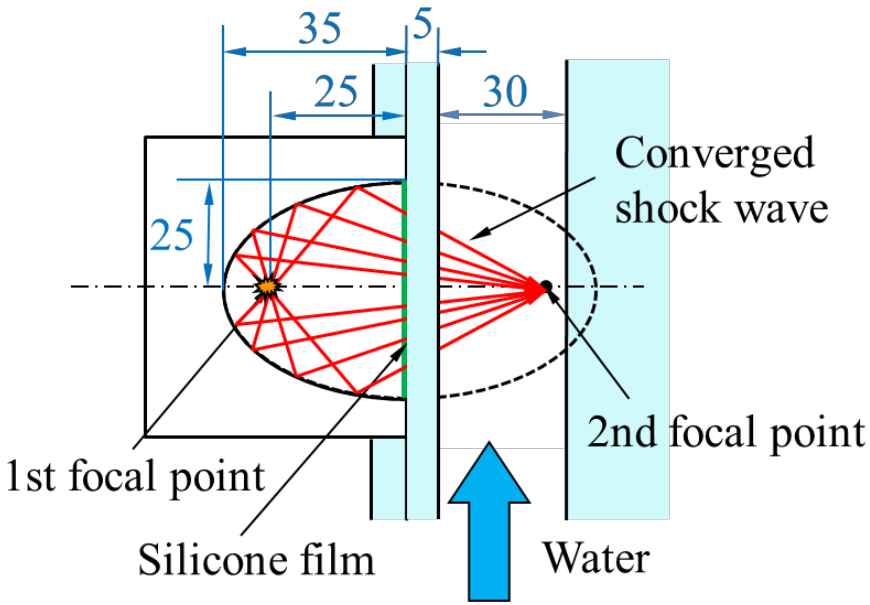
35
5
25
30
25
Converged
shock wave
2nd focal point
1st focal point
Silicone film
Water

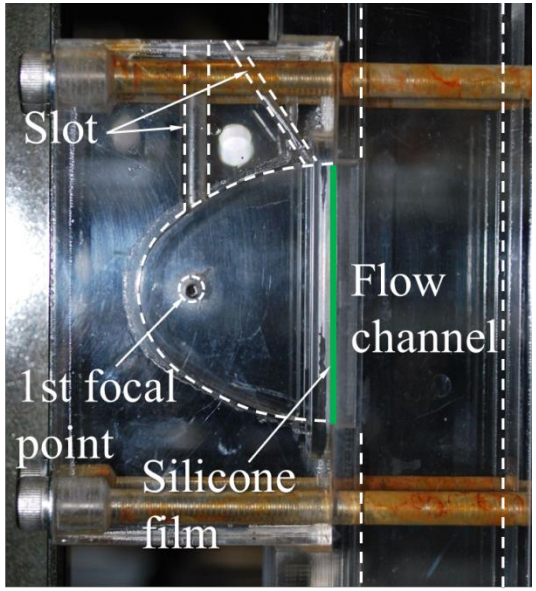
Slot
Flow
channel
1st focal
point
Silicone
film

Fig. 2

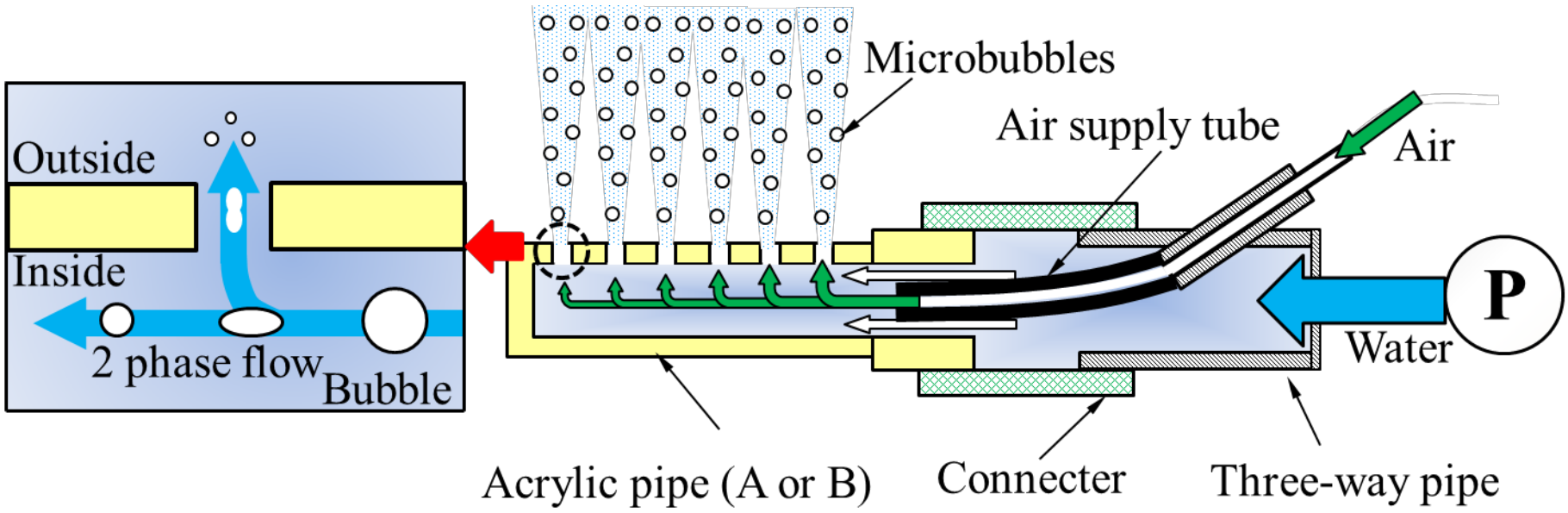
Outside
Inside
2 phase flow
Bubble
Microbubbles
Air supply tube
Air
P
Water
Acrylic pipe (A or B)
Connecter
Three-way pipe

Fig. 3

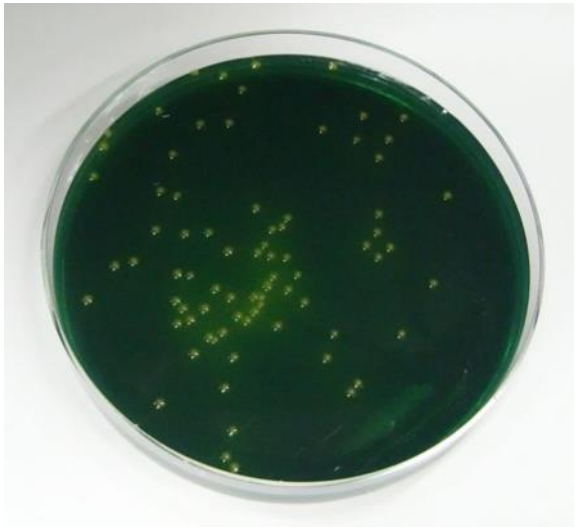

Fig. 4

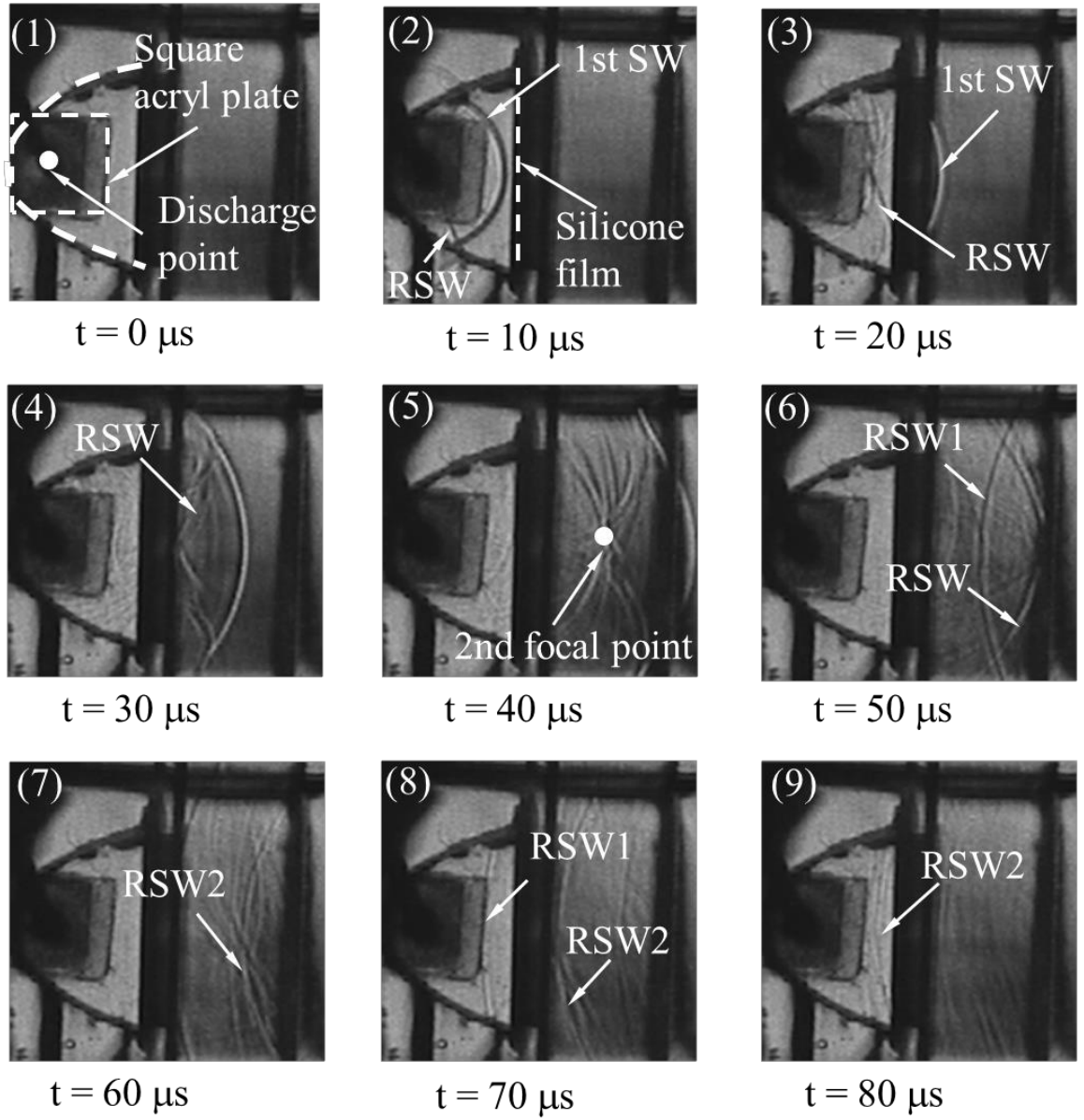
(1)
Square
acryl plate
Discharge
point
t = 0 μs
(2)
1st SW
Silicone
film
RSW
t = 10 μs
(3)
1st SW
RSW
t = 20 μs
(4)
RSW
t = 30 μs
(5)
2nd focal point
t = 40 μs
(6)
RSW1
RSW
t = 50 μs
(7)
RSW2
t = 60 μs
(8)
RSW1
RSW2
t = 70 μs
(9)
RSW2
t = 80 μs

Fig. 5

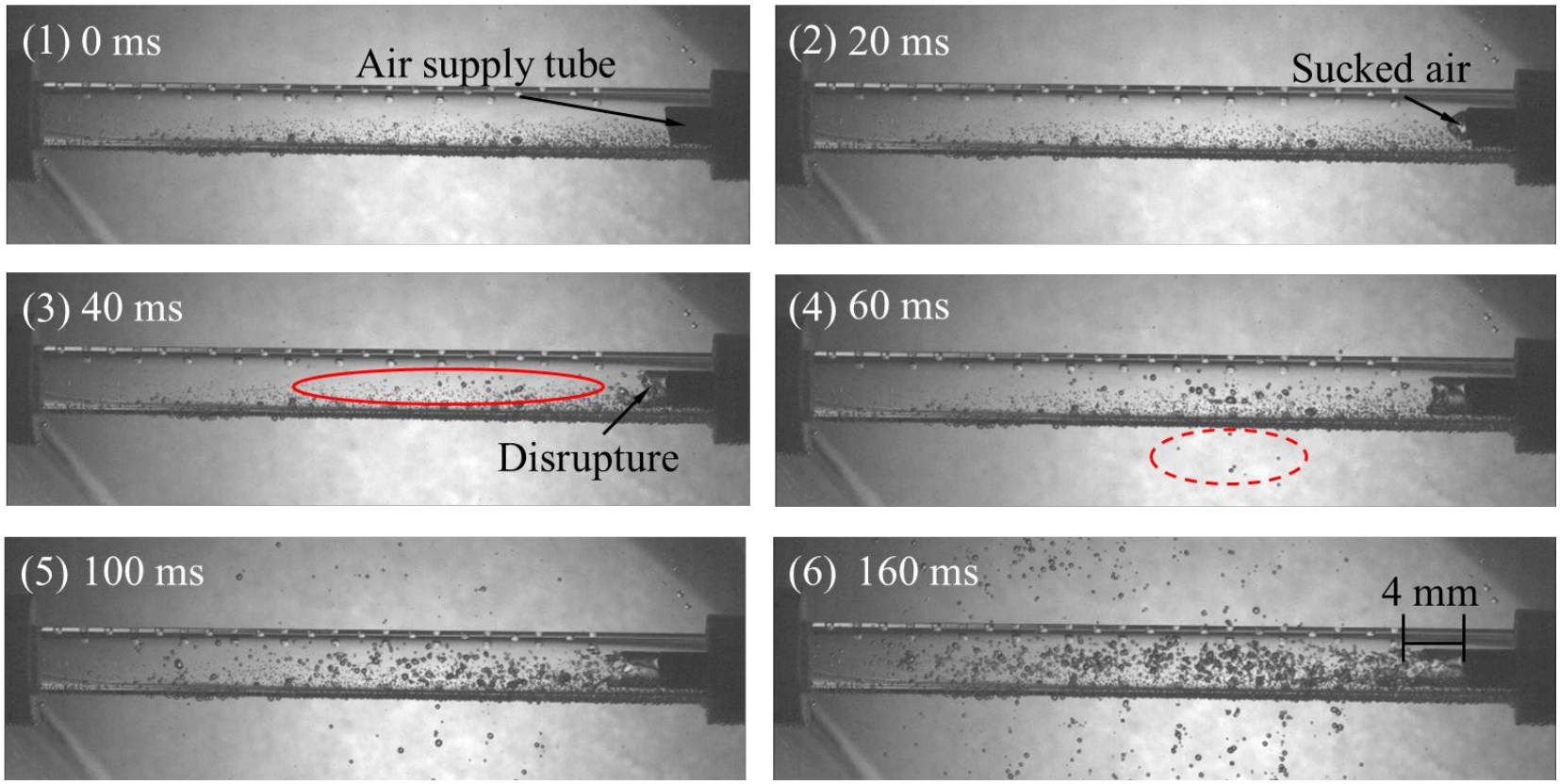
(1) 0 ms
Air supply tube
(2) 20 ms
Sucked air
(3) 40 ms
Disrupture
(4) 60 ms
(5) 100 ms
(6) 160 ms
4 mm

Fig. 6

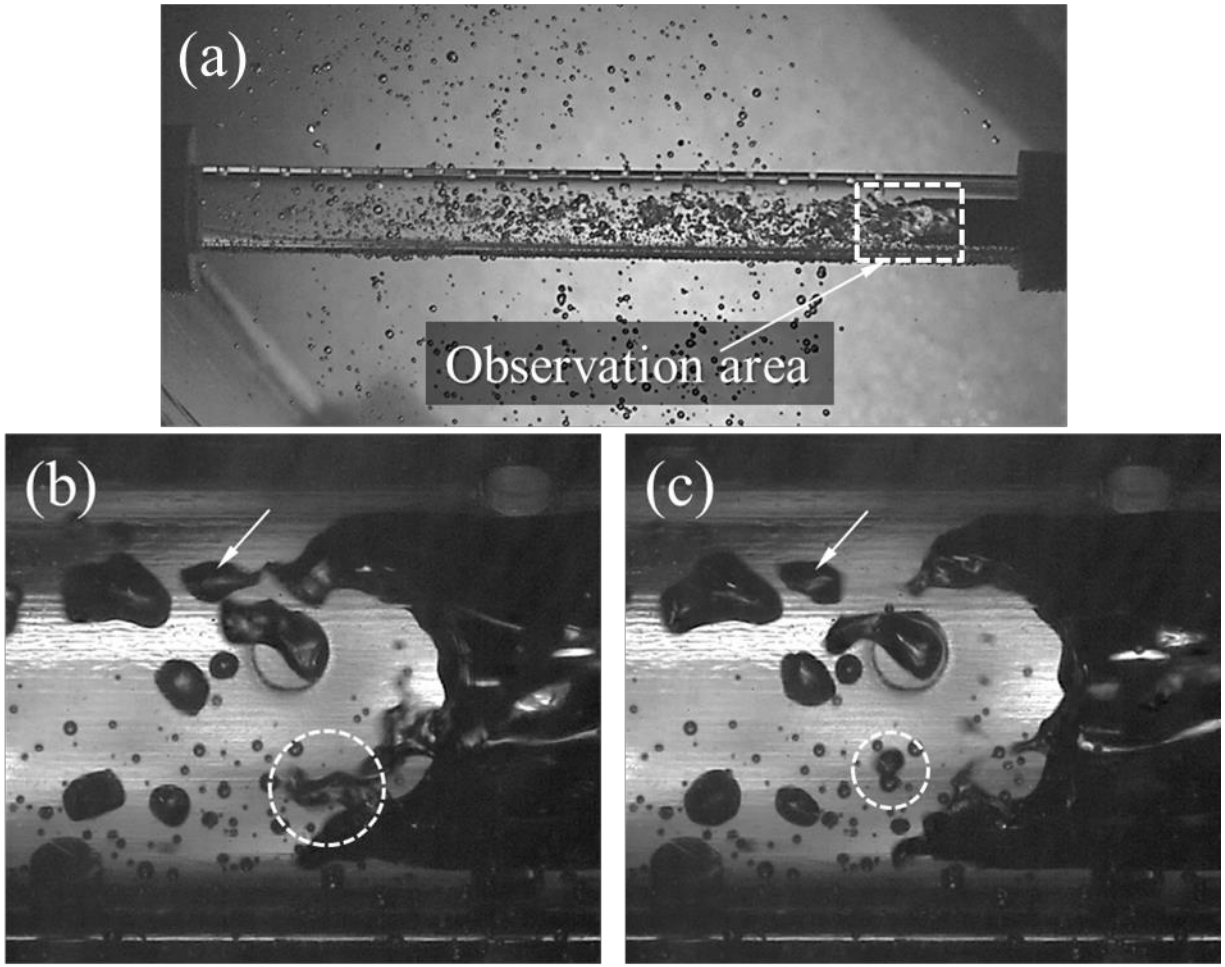

Fig. 7

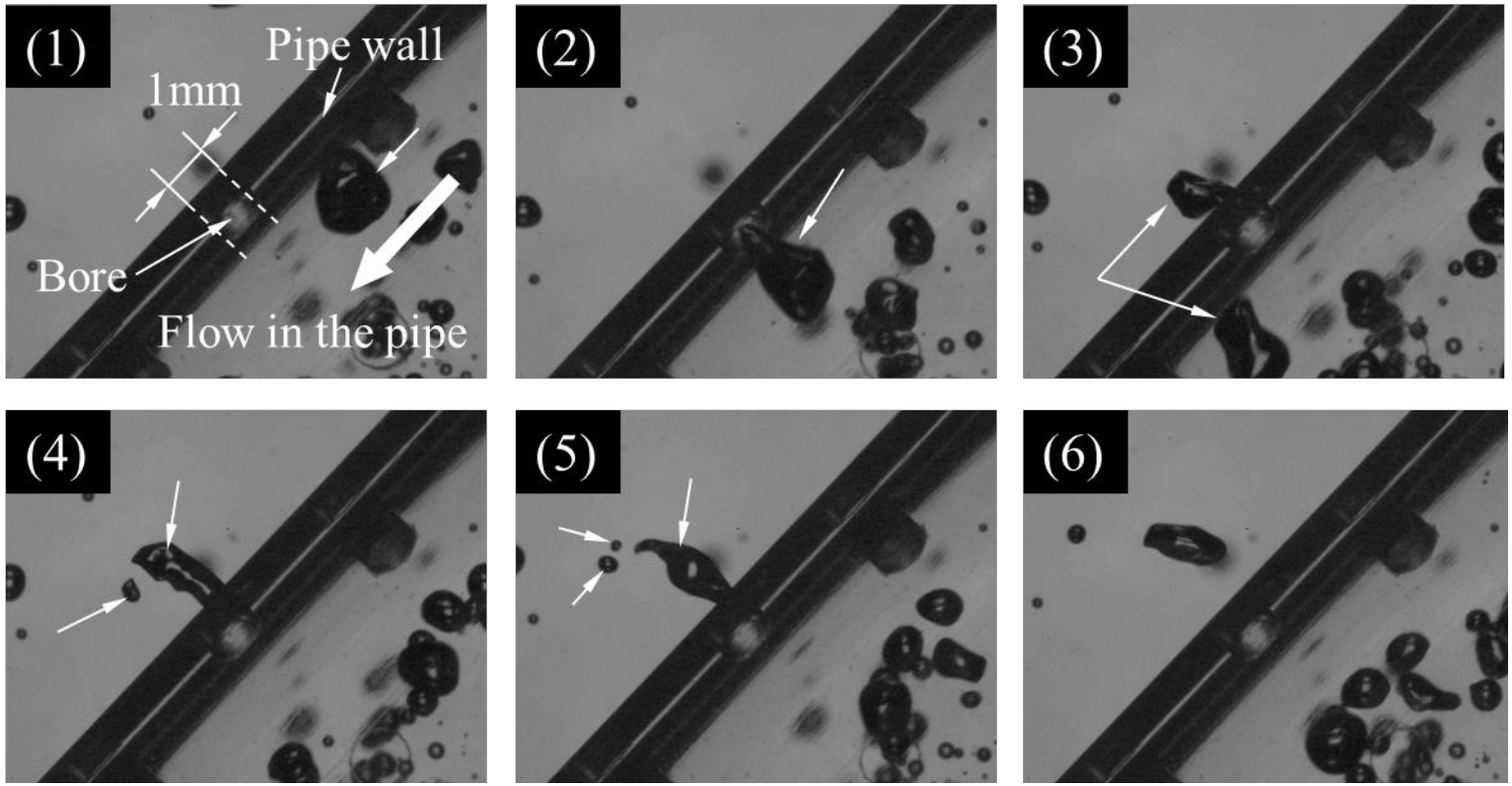

Fig. 8

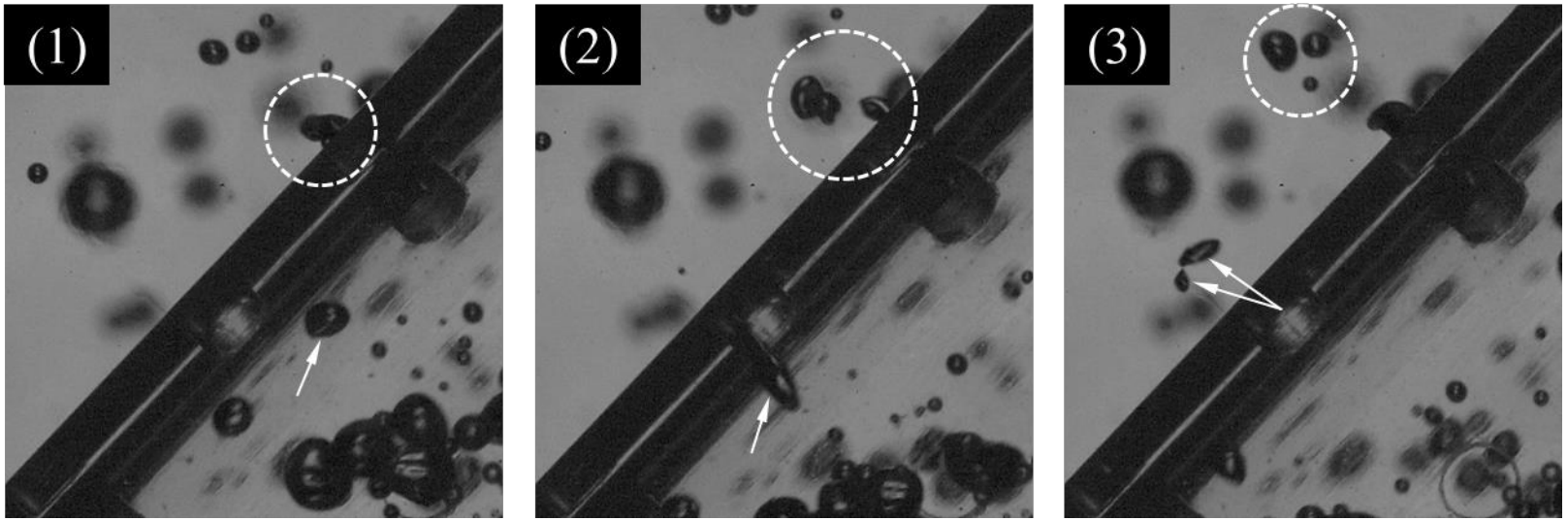

Fig. 9 (a)

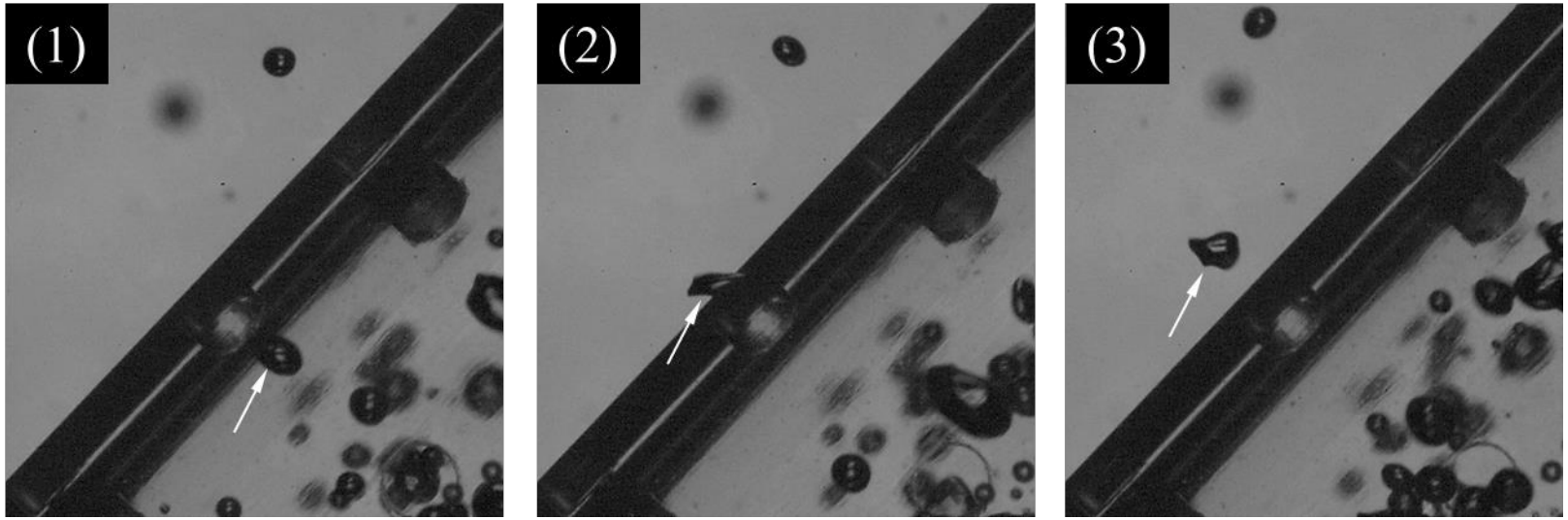

Fig. 9 (b)

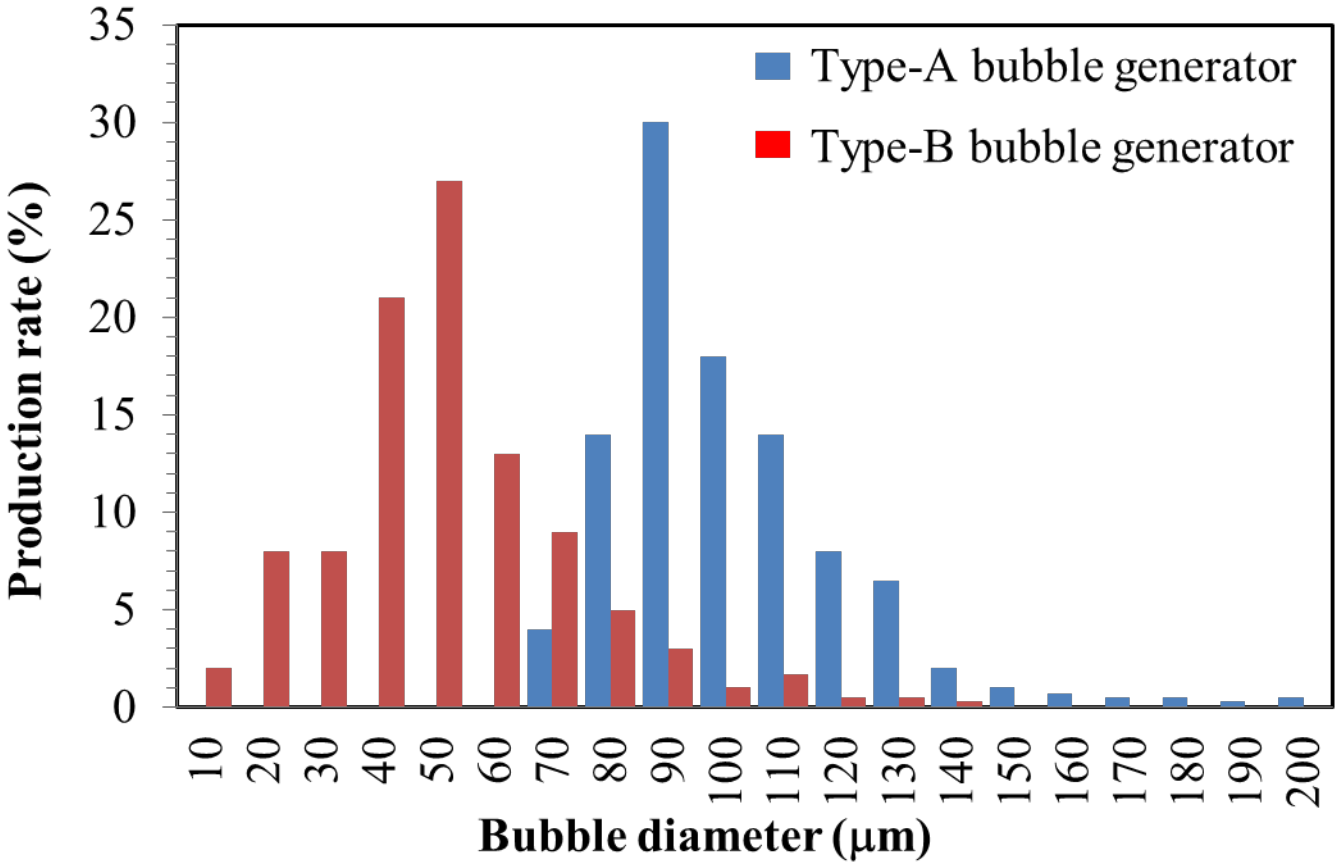
Type-A bubble generator
Type-B bubble generator
Production rate (%)
0
5
10
15
20
25
30
35
10
20
30
40
50
60
70
80
90
100
110
120
130
140
150
160
170
180
190
200
Bubble diameter (μm)

Fig. 10

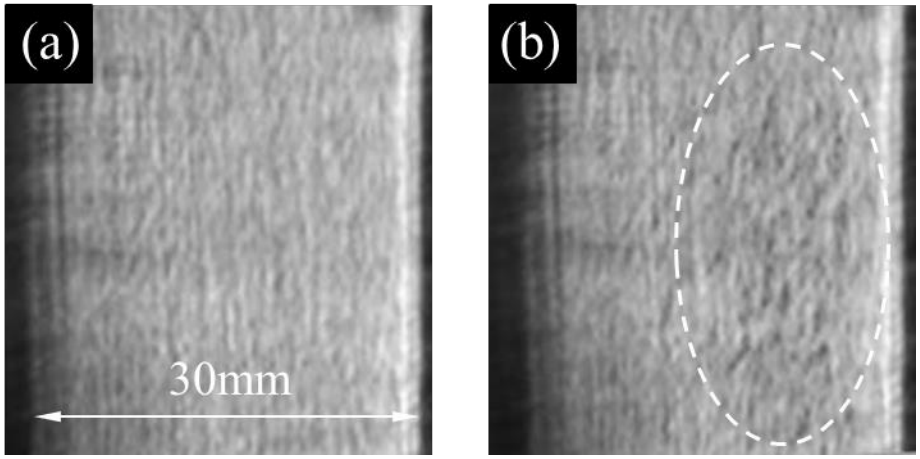

Fig. 11

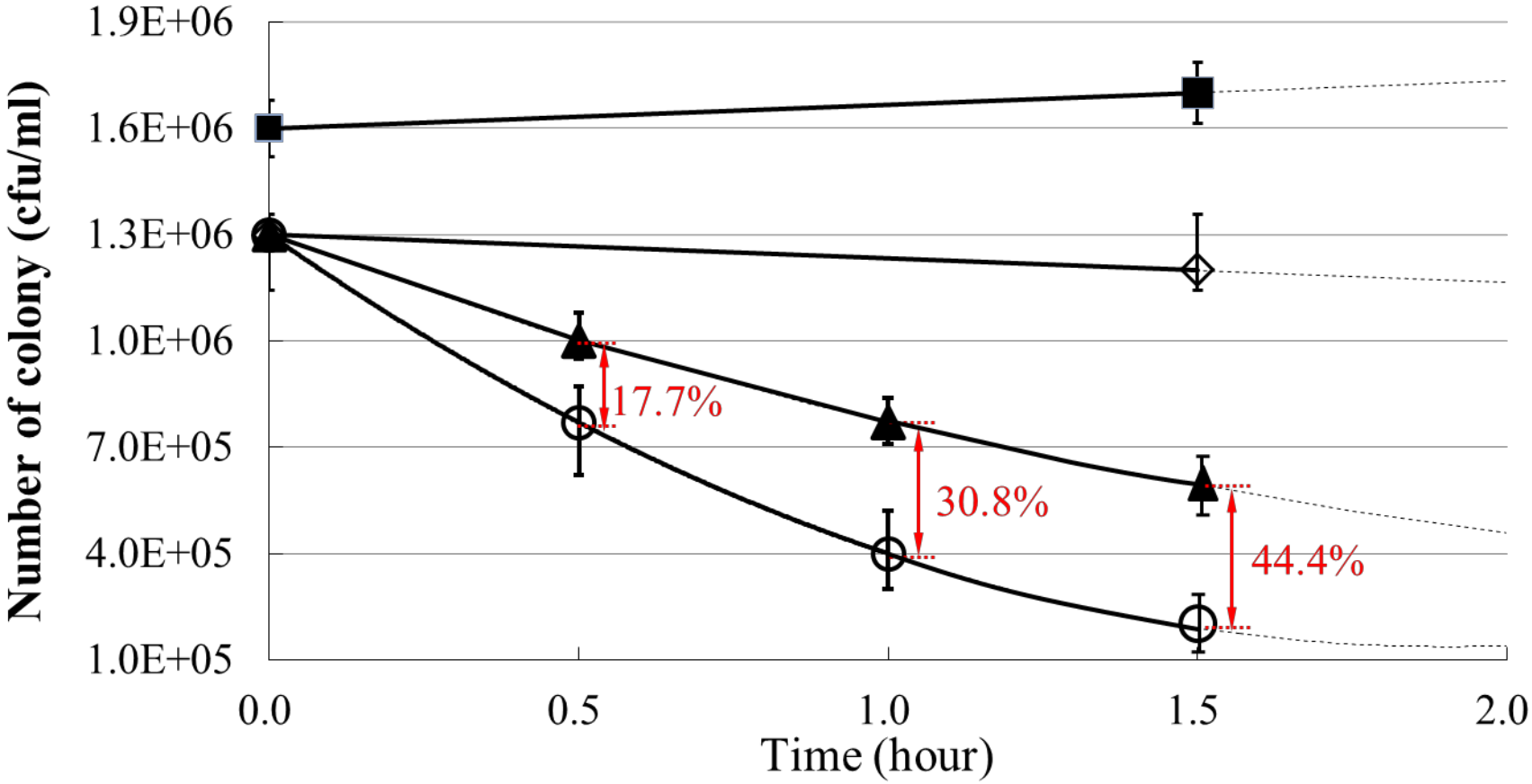
1.9E+06
1.6E+06
1.3E+06
1.0E+06
7.0E+05
4.0E+05
1.0E+05
Number of colony (cfu/ml)
0.0
0.5
1.0
1.5
2.0
Time (hour)
17.7%
30.8%
44.4%

Fig. 12

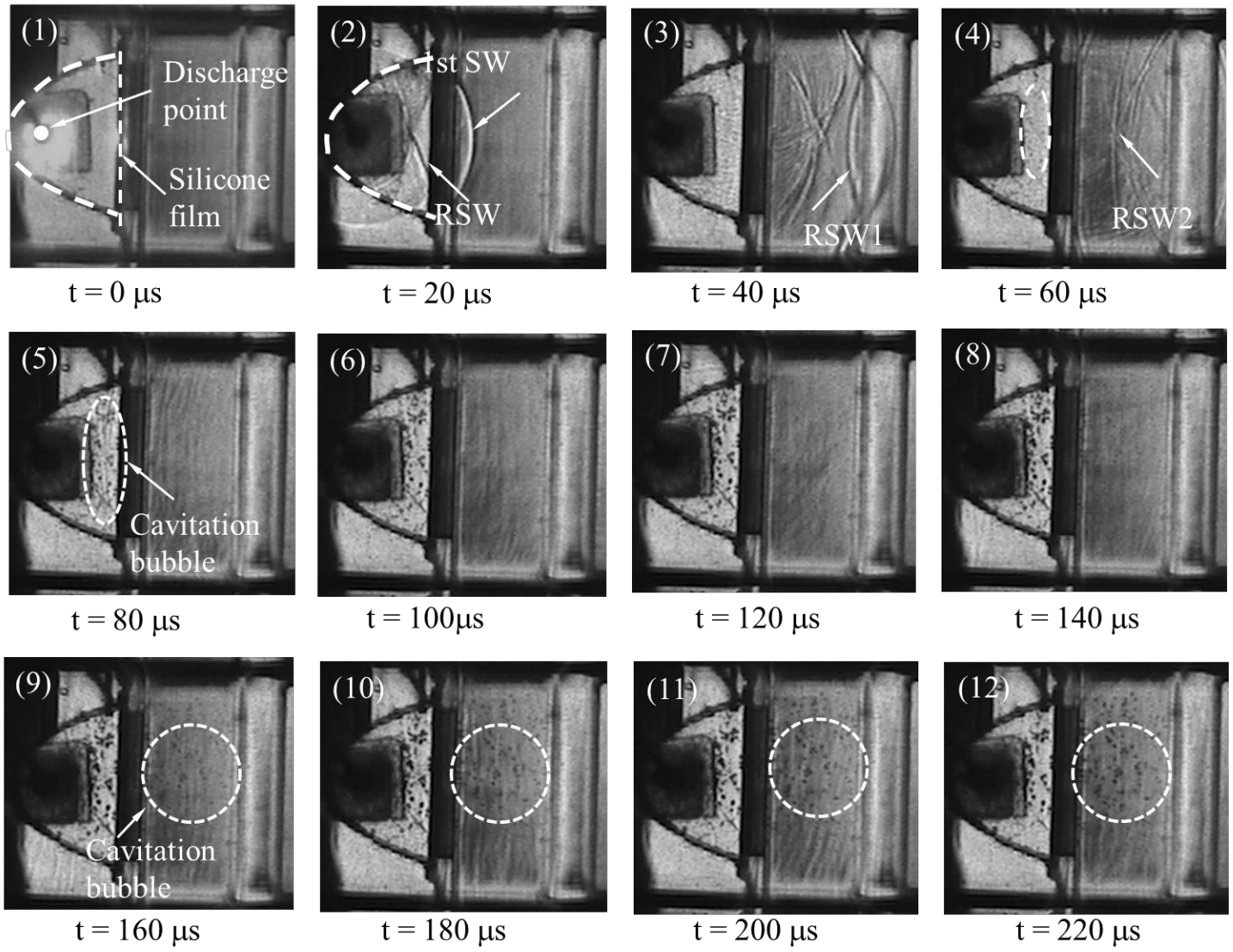
(1)
Discharge point
Silicone film
t = 0 μs
(2)
1st SW
RSW
t = 20 μs
(3)
RSW1
t = 40 μs
(4)
RSW2
t = 60 μs
(5)
Cavitation bubble
t = 80 μs
(6)
t = 100μs
(7)
t = 120 μs
(8)
t = 140 μs
(9)
Cavitation bubble
t = 160 μs
(10)
t = 180 μs
(11)
t = 200 μs
(12)
t = 220 μs

Fig. 13

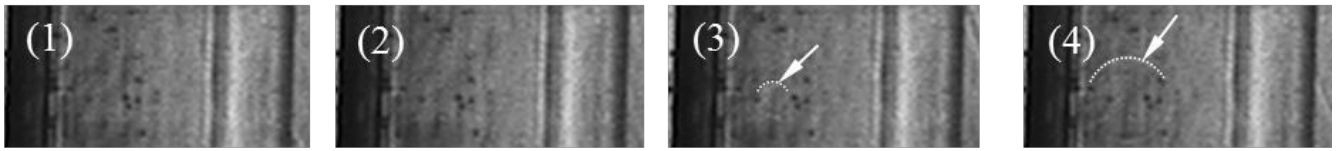

Fig. 14

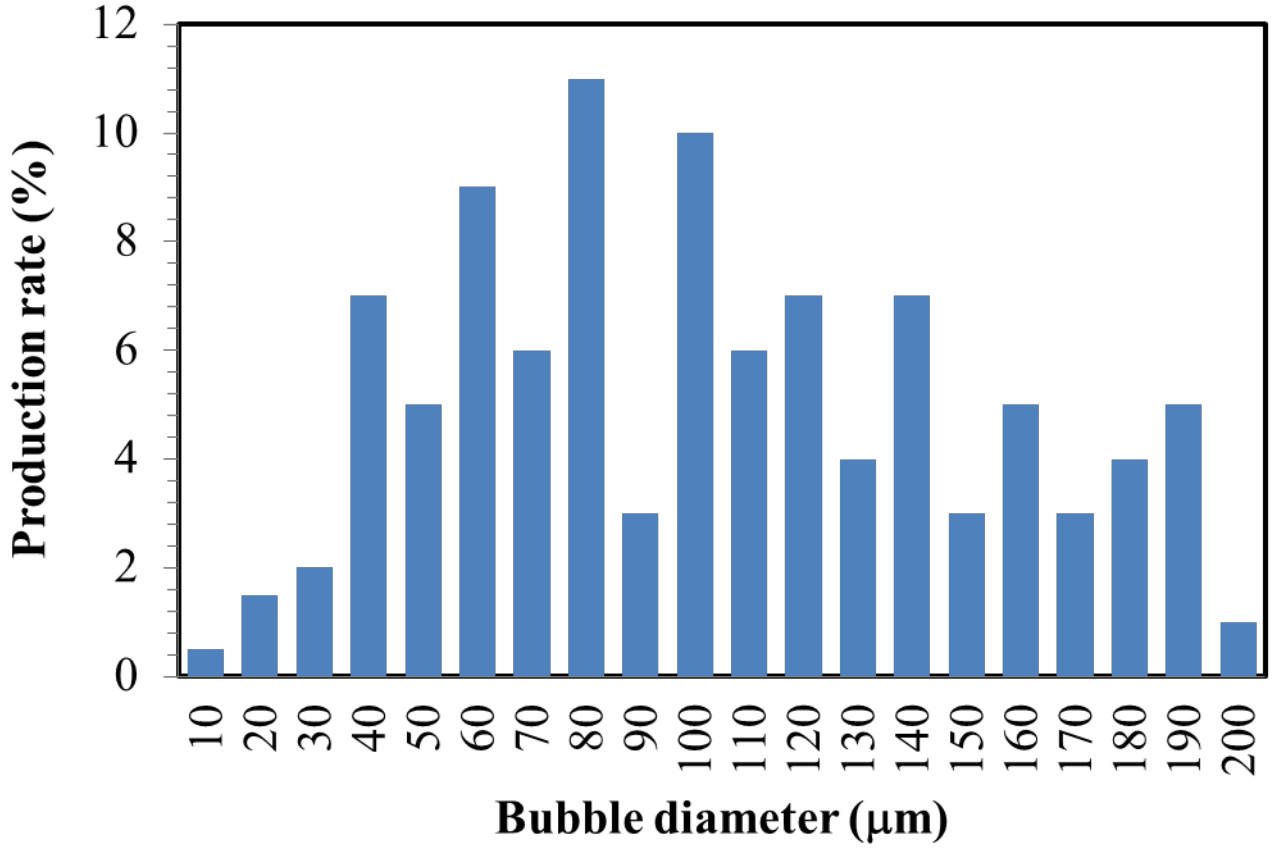
Production rate (%)
0
2
4
6
8
10
12
10
20
30
40
50
60
70
80
90
100
110
120
130
140
150
160
170
180
190
200
Bubble diameter (μm)

Fig. 15